Environmental Science & Technology

Article

pubs.acs.org/est

Systematic Approach to In-Depth Understanding of Photoelectrocatalytic Bacterial Inactivation Mechanisms by Tracking the Decomposed Building Blocks

Hongwei Sun,[†,⊥] Guiying Li,[†] Xin Nie,[†,⊥] Huixian Shi,[†] Po-Keung Wong,[§] Huijun Zhao,[‡] and Taicheng An*[,†]

[†]The State Key Laboratory of Organic Geochemistry and Guangdong Key Laboratory of Environmental Protection and Resources Utilization, Guangzhou Institute of Geochemistry, Chinese Academy of Sciences, Guangzhou 510640, China

[§]School of Life Sciences, The Chinese University of Hong Kong, Shatin, NT, Hong Kong SAR, China

[‡]Centre for Clean Environment and Energy, Griffith University, Gold Coast Campus, QLD 4222, Australia

[⊥]University of Chinese Academy of Sciences, Beijing 100049, China

Supporting Information

ABSTRACT: A systematic approach was developed to understand, in-depth, the mechanisms involved during the inactivation of bacterial cells using photoelectrocatalytic (PEC) processes with *Escherichia coli* K-12 as the model microorganism. The bacterial cells were found to be inactivated and decomposed primarily due to attack from photogenerated H_2O_2. Extracellular reactive oxygen species (ROSs), such as H_2O_2, may penetrate into the bacterial cell and cause dramatically elevated intracellular ROSs levels, which would overwhelm the antioxidative capacity of bacterial protective enzymes such as superoxide dismutase and catalase. The activities of these two enzymes were found to decrease due to the ROSs attacks during PEC inactivation. Bacterial cell wall damage was then observed, including loss of cell membrane integrity and increased permeability, followed by the decomposition of cell envelope (demonstrated by scanning electronic microscope images). One of the bacterial building blocks, protein, was found to be oxidatively damaged due to the ROSs attacks, as well. Leakage of cytoplasm and biomolecules (bacterial building blocks such as proteins and nucleic acids) were evident during prolonged PEC inactivation process. The leaked cytoplasmic substances and cell debris could be further degraded and, ultimately, mineralized with prolonged PEC treatment.

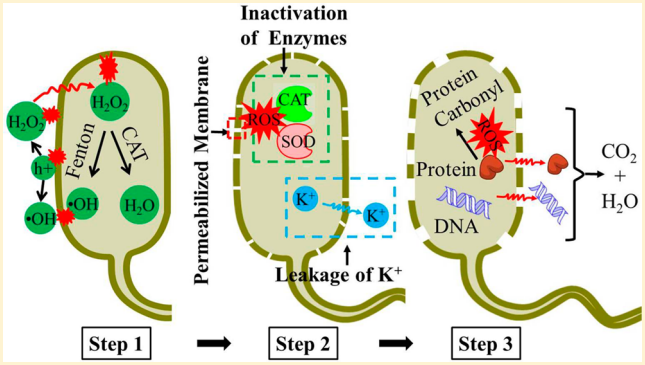

INTRODUCTION

The occurrence of toxic disinfection byproducts, such as trihalomethanes and haloacetic acids, during traditional chlorine disinfection has raised public attention and the necessity to seek safer and more effective processes for drinking water disinfection.[1,2] In 1985, a pioneering work on microbial inactivation with nanosize TiO_2 powder was reported by Matsunaga et al.,[3] and extensive studies on photocatalytic (PC) disinfection have since been reported.[4−9] Regarding the mechanisms of photocatalytic inactivation, it is widely accepted that reactive oxygen species (ROSs), including h^+, e^-, $^{\bullet}OH$, H_2O_2, and $^{\bullet}O_2^-$, were generated and responsible for the inactivation of microorganisms in the PC system. For instance, Cho et al.[10] reported the steady state $^{\bullet}OH$ concentration ($[^{\bullet}OH]_{ss}$) in the TiO_2 PC disinfection system, and a linear relationship between $[^{\bullet}OH]_{ss}$ and the inactivation efficiencies of *E. coli* was found, suggesting $^{\bullet}OH$ to be the predominant inactivation species involved.[11] Kikuchi et al.[12] argued that the major bactericidal species was not $^{\bullet}OH$ but H_2O_2. In their experiments, hydrophilic polytetrafluoroethylene membranes were applied to separate *E. coli* suspension from a TiO_2 thin film, given that neither the half-life nor the half diffusion length of $^{\bullet}OH$ was sufficient to traverse the membrane to attack *E. coli*. Wang et al.[13] also confirmed this conclusion with additional ROSs scavenger experiments in a modified partition system. However, most of the studies regarding the PC inactivation mechanism mainly focused on the specification of the roles of extracellular ROSs. Studies investigating the bactericidal effect of intracellular ROSs are very limited, although intracellular ROSs are believed to be responsible for the oxidative damage of enzymes[14] and DNA,[15] and potentially play very important roles in cell damage during PC inactivation of microorganisms.

Received: May 20, 2014
Revised: July 19, 2014
Accepted: July 25, 2014
Published: July 25, 2014

   dx.doi.org/10.1021/es502471h | Environ. Sci. Technol. 2014, 48, 9412−9419

In addition, the loss of cell membrane integrity of bacterial cells was frequently used as an indicator of the first step of the bactericidal effect,[16] by measuring leakage of intracellular substances such as K^+.[17] In the work of Lu et al., quantum dots of ~5 nm in diameter were observed to be able to penetrate *E. coli* cells exposed to TiO_2 with 20 min illumination, suggesting the destruction of the cell envelope (i.e., cell wall and cell membrane) and the leakage of intracellular macromolecules.[18] The leaked proteins and nucleic acids from bacterial cells are believed to be oxidatively damaged or segmented and further attacked by extracellular- and intracellular-produced ROSs,[14,15] leading to degradation and complete mineralization. However, identifying the details of cell leakage or specific damage to biomolecules, such as proteins and nucleic acids, was rarely attempted in PC inactivation systems.

The photoelectrocatalytic (PEC) process has recently been confirmed to significantly improve the efficiency of PC degradation of organic pollutants and inactivation of bacteria. In comparison to the photocatalytic system, the PEC system immobilizes a catalyst onto a conducting substrate and uses it as the photoanode. It allows us to apply a potential bias to the photoanode. The applied potential bias serves as an external driving force that can timely remove the photogenerated electrons from conduction band to external circuit and then to auxiliary electrode. The improved efficiency is due to the effectively suppressed photogenerated electron and hole recombination,[19−21] especially using a TiO_2 nanotube array as a photoelectrode in the PEC system.[22] However, to the best of our knowledge, the details regarding the mechanism of bacterial inactivation by PEC has not been investigated. Therefore, in this study, a systematic approach was developed to understand, in-depth, PC and PEC bacterial inactivation mechanisms by tracking the decomposed building blocks and the intracellular enzymatic defensive activities. The aims of the study were (1) to verify the contribution of ROSs and identify the dominant species in PEC inactivation systems; (2) to quantify levels and identify potential roles of intracellular ROSs during PEC disinfection; (3) to clarify the changes in cell membrane permeability utilizing fluorescent staining, enzyme activity assays, and direct observation by scanning electronic microscope (SEM); and (4) to investigate the leakage and oxidative damage of intracellular biomolecules during PEC inactivation.

EXPERIMENTAL SECTION

Reaction Apparatus. The PEC, PC, and electrochemistry (EC) inactivation experiments were all conducted in a 50 mL three-electrode photoelectrochemical bulk reactor with a quartz window, as shown in Figure S1 in the Supporting Information (SI). The photoanode, a piece of Ti foil with highly oriented TiO_2 nanotube array (15 mm × 15 mm), was used in this work. Details regarding the preparation procedure were reported in our previous study,[23] and the brief physical and chemical information on the TiO_2 nanotubes was provided in the SI. Platinum foil and a saturated Ag/AgCl were served as counter and reference electrodes, with 0.2 M $NaNO_3$ as electrolyte under a constant anode bias potential of +1.0 V versus Ag/AgCl. The illumination source consisted of four UVA light-emitting diodes (LED lamps) with a maximum emission at 365 nm and the intensity adjusted to 27 mW cm^{-2}.

Procedure for Bacterial Inactivation. The bacteria suspension of *Escherichia coli* K-12 (Coli Genetic Stock Center, Yale University, USA) was prepared following the same procedure as our previous report.[24] Unless otherwise stated, the initial bacteria population was 1.1 × 10^7 colony forming units per milliliter (CFU mL^{-1}). Fifty mL of the prepared *E. coli* suspension (in the early stationary phase) was employed to conduct the inactivation experiments in the bulk PC reactor. Samples were collected at regular intervals, and the culturable bacterial density was determined by a plate count method.[25]

Intracellular ROS Assays. The fluorescent probe 2′,7′-dichlorodihydrofluorescein diacetate (DCFH-DA) was adopted to monitor the intracellular ROSs levels.[26] The nonfluorescent probe DCFH-DA can enter bacterial cells where it can be hydrolyzed by intracellular esterase and further oxidized by intracellular ROSs to form fluorescent 2′,7′-dichlorofluorescein (DCF). The detailed protocol of the fluorescent assay is provided in the SI, and the mechanism is illustrated in Figure S2.

Enzyme Activity Assays. To measure the activity of catalase (CAT) and superoxide dismutase (SOD), bacterial cells were harvested, and the protein content was extracted following inactivation treatments. Details of the assay procedures can be found in the SI. For the β-D-galactosidase activity assay, 1 mL of 16-h incubated *E. coli* suspension in nutrient broth was cultured in 100 mL of nutrient broth containing 1 mM isopropyl β-D-thiogalactopyranoside (IPTG) and incubated at 37 °C, 200 rpm for 4 h to induce the synthesis of β-D-galactosidase. Induced cells were harvested and resuspended in 0.2 M $NaNO_3$ for inactivation. Aliquots of 0.5 mL samples were collected at regular time, and the hydrolysis rate of *o*-nitrophenyl-β-D-galactopyranoside (ONPG) was determined in cells with and without SDS/chloroform permeabilization. The ratio of the latter to the former reflects the membrane permeability. Details of the assay procedures are also summarized in the SI.

Fluorescent Staining, K^+ Leakage, SEM Observation, and Total Organic Carbon (TOC) Content Analysis. Bacterial cells were stained with LIVE/DEAD BacLight Bacterial Viability Kit (Molecular Probes, USA) to monitor cell membrane integrity with fluorescence microscope, following the kit protocols. Bacterial cells with intact cell membranes (live) were stained green, while those with damaged cell membranes (dead) were stained red.

Samples of 5 mL were collected from the inactivation solution at regular intervals and filtered through 0.22 μm filter to remove bacterial cells; the concentration of K^+ was then determined using inductively coupled plasma-atomic emission spectroscopy (VISTA ICP-AES Pro, USA). The preparation procedure for SEM samples was similar to the description in our previous work,[27] and details can be found in the SI. The TOC contents of inactivated bacteria suspensions were measured by a TOC analyzer (Shimadzu TOC-VCPH, Kyoto).

Protein Leakage and Oxidative Damage Assay. For protein leakage assay, the bacterial cells of 8 mL suspension were harvested, followed by protein extraction with 40 μL B-PER reagent (Pierce Biotechnology, USA). The protein concentration was measured by Bradford assay (SK3041, Sangon Biotech, Shanghai, China). Leakage of protein was confirmed with sodium dodecyl sulfate polyacrylamide gel electrophoresis (SDS PAGE) using the extracted protein samples from 10^8 CFU mL^{-1} bacterial suspensions. Details of the procedures are described in the SI.

For the protein oxidative damage assay, a 5 mL treated suspension of *E. coli* (10^8 CFU mL^{-1}) was lysed by sonication with 50 μL of 100 mM phenylmethanesulfonyl fluoride and 5

μL of 5% butylated hydroxytoluene. The lysate was concentrated by ultrafiltration to 10 μg protein mL^{-1}, and the oxidative protein levels were measured using an OxiSelect Protein Carbonyl ELISA Kit (STA-310, Cell Biolabs, USA), following the protocol provided by the manufacturer.

Chromosome DNA Leakage Assay. *E. coli* in 10 mL suspensions (10^8 CFU mL^{-1}) at various intervals were harvested, and the chromosomal DNA was extracted using an Ezup Column Bacteria Genomic DNA Purification Kit (SK8255, Sangon Biotech, Shanghai, China). DNA agarose gel electrophoresis (AGE) was performed with 0.6% agarose gel at 100 V for 45 min in 1 × TAE buffer to verify DNA leakage.

RESULTS AND DISCUSSION

Inactivation Performances and the Contribution of Various ROSs. The viabilities of *E. coli* during PEC, PC, and EC inactivation are shown in Figure 1a. PC and EC showed no inactivation effect during 60 min treatment, while PEC inactivated all bacterial cells within 45 min. The inactivation efficiency was enhanced significantly by means of suppressing the recombination of photogenerated h^+ and e^- in the PEC system, compared with that in the PC system. The inactivation efficiencies followed the order of PEC > PC > EC (Figure S3) when the experiments were carried out in a thin-layer reactor, as shown in Figure S4.

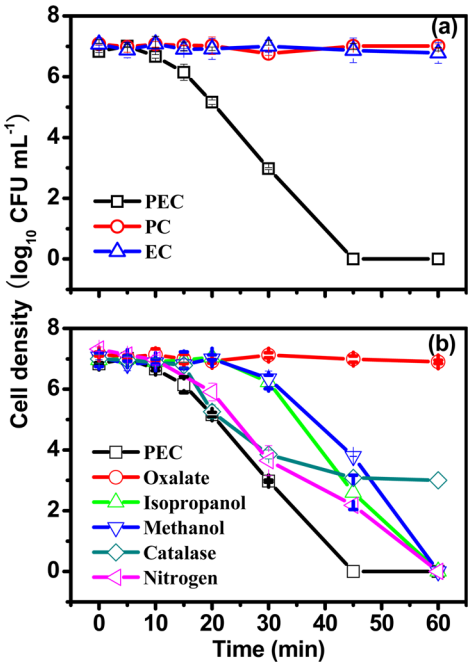

Figure 1. (a) Culturable cell density in logarithm of *E. coli* during PEC, PC, and EC inactivation; (b) ROSs scavenger experiments in PEC inactivation system, where the concentrations of the scavengers are as follows: 1 mM sodium oxalate (oxalate), 1 mM methanol, 1 mM isopropyl alcohol, and 0.05 μM catalase.

Scavenging experiments were also conducted to identify which ROSs are primarily responsible for the inactivation in the PEC system (Figure 1b). The addition of 1 mM sodium oxalate can completely suppress the inactivation efficiencies, by eliminating valence band ROSs including h^+ and its derivatives such as $^{\bullet}OH$ and H_2O_2. When $^{\bullet}OH$ was removed, either by 1 mM methanol or isopropyl alcohol, the inactivation performance was depressed by ~3−4 log. Live bacteria cells remained until 45 min, but the complete inactivation was achieved when the PEC process continued for 60 min. The addition of 50 nM CAT could inhibit the bactericidal effect, especially at the later phase of PEC treatment, with ~3 log live cells remaining until 60 min; whereas purging with nitrogen during the PEC process only slightly decreased the bactericidal effect, implying that dissolved oxygen and its reduced derivative $^{\bullet}O_2^-$ were not important bactericidal species in this PEC system. Therefore, it can be concluded that valence band ROSs were dominant in this PEC system rather than conduction band ROSs. Among the valence band ROSs, h^+ seems unlikely to be the major species to directly inactivate bacteria, because it is generated on the surface of the anode and cannot move, thus its contact with the bacterial cells is rather limited. The bactericidal effect of $^{\bullet}OH$ was also limited by its short life-span (~300−500 μs).[12] However, H_2O_2 is more stable with a half-life of several days in pure water. Although biodegradation and photo-oxidation may reduce the half-life to minutes (Material Safety Data Sheet ACC# 11189, Fisher Scientific, http://www.coleparmer.com/Assets/Msds/11189.htm), it is still sufficient for H_2O_2 to diffuse into the suspension. More importantly, H_2O_2 can permeate through cell membranes,[28] causing damage inside the bacterial cells. It is known that H_2O_2 is more stable under acidic conditions, while the decomposition of H_2O_2 can be accelerated under alkaline conditions. Therefore, the effect of pH value on the production of H_2O_2, and subsequently on PEC inactivation, was further investigated (Figure S5a). Compared to a more neutral pH (pH = 6.25), the inactivation efficiency decreased under alkaline conditions (pH = 7.39 and 8.35) and elevated under acidic conditions (pH = 4.31). The concentrations of H_2O_2 ($[H_2O_2]$) and the steady state $^{\bullet}OH$ ($[^{\bullet}OH]_{ss}$) were measured according to the methods reported,[10,29] and the results are summarized in Figures S5b and S5c. In conclusion, $[H_2O_2]$ were higher at pH 4.31 and much lower at pH 8.35, compared to pH 6.25, which coincides with the inactivation performance. Higher $[H_2O_2]$ under acidic conditions may be due to less decomposition and more generation of H_2O_2, according to eq 1,[12] and vice versa under alkaline conditions. However, no measurable variance of $[^{\bullet}OH]_{ss}$ was observed at different pH values, indicating that H_2O_2, rather than $^{\bullet}OH$, was the most effective bactericidal species in this PEC system. In addition, the electrostatic forces between negatively charged *E. coli* cells[30] and TiO_2 with isoelectric points at pH = 6.8[31] might also be partly responsible, as well as the synergism between pH-related stress and PEC disinfectants. Notably, the dominant bactericidal agent in this work was quite different from PC disinfection using suspended nanoparticles, where the roles of $^{\bullet}OH$ and h^+ may be more important because of the increased contact events between bacteria and catalyst particles.[11]

$$^{\bullet}O_2^- + e_{cb}^- + 2H^+ \rightarrow H_2O_2 \quad (1)$$

Intracellular ROSs Levels and Antioxidative Enzyme Activities. As mentioned, the bactericidal effect may be partly due to the endogenous damage caused by intracellular ROSs attacks; therefore, the intracellular ROSs levels were also monitored by fluorescent probe DCFH-DA in response to the accumulation of the extracellular ROSs (Figure 2a). DCFH-DA has been widely used for the detection of intracellular ROSs such as H_2O_2 and $^{\bullet}OH$.[32] During PEC inactivation, intracellular ROSs levels increased as soon as the inactivation process was started and continued to increase until 20 min. The decrease of fluorescent intensity after 20 min indicated the loss of bacterial

dx.doi.org/10.1021/es502471h | Environ. Sci. Technol. 2014, 48, 9412−9419

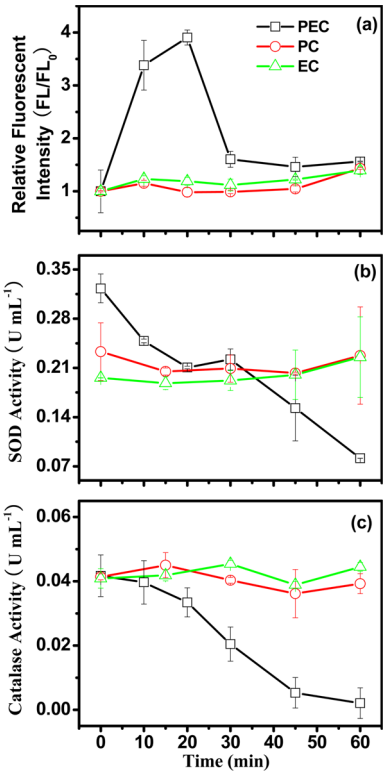

Figure 2. (a) Intracellular ROSs levels shown by relative fluorescent intensity of probe DCFH-DA, where the fluorescent intensity was normalized by initial fluorescent intensity at 0 min (FL/FL_0); (b) SOD and (c) catalase activity during PEC, PC, and EC inactivation processes. The enzyme activities were stated as unit activity per milliliter (U mL^{-1}) of bacterial suspension (1.1×10^7 CFU mL^{-1}).

esterase activity and the leakage of fluorescent product, considering that ~99% of the bacterial cells were inactivated after 20 min (Figure 1a). However, no increase of intracellular ROSs levels was observed during PC or EC treatment, due to their poor oxidative capacity. As discussed above, H_2O_2 has been recognized to be the major bactericidal reagent in this PEC system, rather than $^{\bullet}OH$. However, H_2O_2 was much less reactive than $^{\bullet}OH$ and can be eliminated by the bacterial catalase, rendering it incapable of inactivating the bacteria. The detected increase of intracellular ROSs during the PEC process suggests that H_2O_2 may penetrate the cells and generate more reactive $^{\bullet}OH$ through Fenton reaction[33] or Harber-Weiss reaction,[12] according to eqs 2 and 3

$$Fe^{2+} + H_2O_2 + H^+ \rightarrow Fe^{3+} + {}^{\bullet}OH + H_2O \quad (2)$$

$$^{\bullet}O_2^- + H_2O_2 \rightarrow {}^{\bullet}OH + OH^- + O_2 \quad (3)$$

where $^{\bullet}O_2^-$ would be constantly generated by organisms through a variety of pathways such as aerobic respiration and UV irradiation by means of photosensitization;[12,28] and a free iron pool of about 20 μM, contained in *E. coli* cells without integrated into proteins, was also available for the Fenton reaction *in vivo*.[34]

The increased ROSs, such as $^{\bullet}O_2^-$ and H_2O_2, in bacterial cells would normally be scavenged by antioxidative enzymes, such as SOD and CAT, that catalyze the conversion and detoxification of $^{\bullet}O_2^-$ and H_2O_2, respectively.[28,35,36] Thus, the SOD and CAT activities during bactericidal treatment were also monitored, and the results are shown in Figures 2b and 2c. For the PEC process, the decrease of both SOD and CAT activities was observed after 10 min of inactivation and continued thereafter. It was reported that SOD and CAT would be oxidatively damaged, and the enzyme activity was lost when the bacterial cells were attacked by free radicals, resulting in the fragmentation of proteins, the release of ions, and the generation of protein carbonyl derivatives.[37] Thus, the rapidly elevated intracellular ROSs levels, at the initial stage of PEC, were responsible for the decrease of SOD and CAT activity, indicating that the attack potential of generated ROSs overwhelmed the antioxidative capacity of these two bacterial enzymes. The loss of SOD and CAT activities, in return, accelerated the accumulation of ROSs, and then the loss of cell cultivability, as shown in Figure 1a. Neverthless, the enzyme activities during PC and EC did not vary considerably during 60 min of treatment, coresponding to the limited intracellular ROSs levels in these two processes.

Membrane Permeability Changes and Leakage of K^+. The oxidative stress on bacterial cells generally results in lipid peroxidation of cell membranes,[38,39] which might be responsible for the cell membrane permeability changes. Therefore, the bacterial membrane integrity during PEC process was first monitored by fluorescent staining using Live/Dead BacLight Bacterial Viability Kit. The microscopic images of stained bacteria are shown in Figure S6. All the untreated cells with intact cell membranes were stained green, and red fluorescent staining cells with compromised cell membranes increased with prolonged PEC treatment. All bacterial cells were stained red at 60 min, suggesting that the membrane integrity of all the cells was lost. In contrast, the bacterial cells in EC and PC systems did not show any change, with all cells remaining green after 60 min (Figure S7). Notably, the permeabilization of cells in PEC seemed slower than inactivation. For example, at 30 min, when ~99.99% of the cells were inactivated, about half of the cells were still stained green. Similar results were also obtained by previous works.[4,40] In addition, Berney et al.[40] also observed the increased uptake of green fluorescent dye SYTO 9 along with disinfection. Thus, it needs more red fluorescent dye (PI) to quench the green dye. In other words, the uptake of PI by permeabilized membranes perhaps took place earlier than it was indicated by the red stained cells, which can be demonstrated by some orange cells in the images. The mechanism of increased membrane permeability could be that, as previously reported by Bosshard et al.,[41] membrane associated proteins such as enzymes of respiratory chain and ATPase were inactivated quickly, and thus the bacterial energy metabolism was insufficient to maintain membrane potential. Loss of membrane potential subsequently caused the increased membrane permeability as it is important for substrate transport processes across membranes.

To further reveal the cell membrane permeability of the treated cells, β-D-galactosidase activity assay, which catalyzes the hydrolysis of o-nitrophenyl-β-D-galactopyranoside (ONPG) to produce yellow colored o-nitrophenol (ONP), was employed. For intact cells, the permeability of ONPG was very limited because of the barrier posed by the cell membrane and the availability of lactose permease.[42] In the PEC system (Figure 3), the ONPG hydrolysis rate in permeabilized cells (where ONPG have free-access to the enzyme) decreased quickly from 33.4 to 1.2 nmol min^{-1} mL^{-1} within the initial 20 min and then slowly decreased to 0 nmol min^{-1} mL^{-1} after 60 min, which indicated the β-D-galactosidase was inactivated gradually by PEC, coincided with the bacterial death (Figure 1a).

dx.doi.org/10.1021/es502471h | Environ. Sci. Technol. 2014, 48, 9412−9419

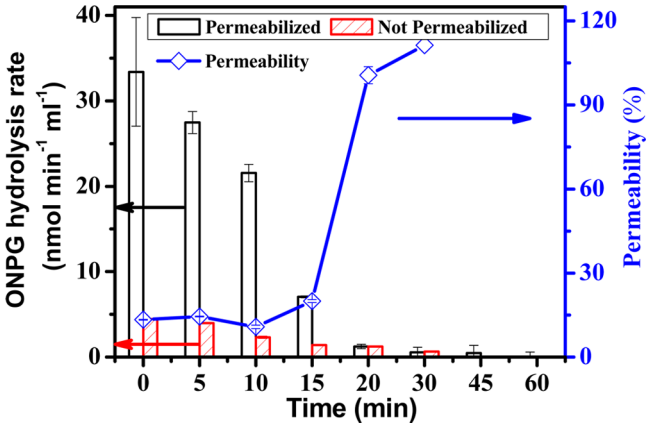

Figure 3. β-D-Galactosidase activity and membrane permeability of the PEC treated bacteria determined by ONPG hydrolyzation assay.

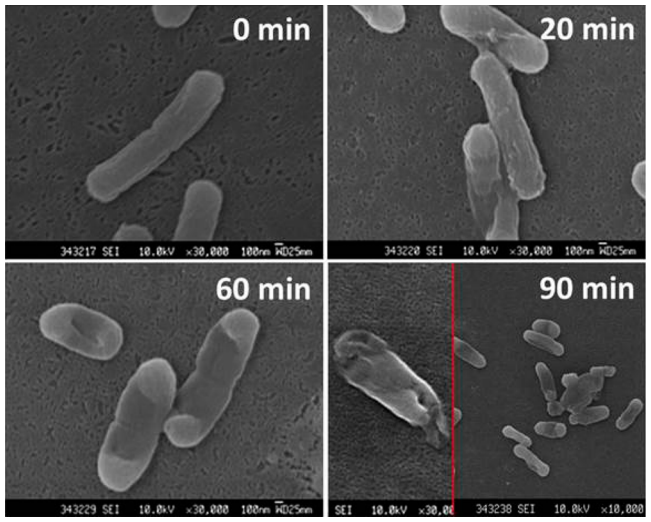

Figure 4. SEM images of bacteria inactivated by PEC process for 0, 20, 60, and 90 min.

Comparatively, the ONPG hydrolysis rate in cells without permeabilization was much lower at the beginning, due to limited diffusion of ONPG across the cell membrane. The cell membrane permeability changed slightly until 10 min of PEC inactivation. This may be explained by a counteraction between the increased permeability and the decreased permease activity due to inactivation of ATPase,[41] on ONPG transport across the membrane. Permeability increased after 10 min, in particular during 15−30 min, to maximum. K^+ leakage during the PEC inactivation was also used to further confirm this conclusion (Figure S8), where the elevated K^+ leakage took place during 15−30 min. Relatively high concentrations of intracellular K^+ were generally maintained in intact bacterial cells. The leakage of K^+ from the cytoplasm indicated the elevated permeability of cell membranes.[17] In contrast, neither total nor intracellular β-D-galactosidase activity fluctuated significantly during PC and EC processes, as with ONPG permeability (Figure S9). To conclude, the membrane permeabilization took place mainly in 15−30 min, coincided with the exponential disinfection period, after ∼80% bacterial cells were inactivated (at 15 min); but yet it may not be appropriate to conclude that membrane damage occurred later than culturability loss, because it was reported that oxidative bursts during aerobic incubation (adopted for culturability assay in this work) may result in lower CFU.[40]

Bacterial Decomposition and Biomolecules Leakage. The damage of cell membranes was directly observed by SEM, and the destruction of bacteria cells was measured by the leakage of various biomolecules. As shown in Figure 4, the untreated *E. coli* cells exhibited plump rod shapes with intact cell envelopes. Rougher cell surfaces, with wrinkles and even collapse, were observed for some cells after 20 min of treatment, indicating the partial decomposition of cell envelope and the leakage of cytoplasm. All cells were shriveled with most of the intracellular substances leaked when PEC treatment was prolonged to 60 min, and this appearance was more severe at 90 min. Notably, some of the cells showed only the cell envelope debris with many hollows and holes, as illustrated in Figure 4. In contrast, the cells treated by EC retained cell envelope integrity, even after 120 min. PC treatment did not result in any obvious damage to the cells until 120 min, when the sunken areas were observed on some bacterial cells (Figure S10).

The above SEM images motivated us to check the leakage of intracellular substances, the building block of bacteria, such as proteins and nucleic acids. The protein content of 8 mL PEC-treated cells (10^7 CFU mL^{-1}) reduced from 182.0 to 4.5 μg mL^{-1} after 90 min of treatment (Figure S11), which demonstrated the leakage of protein from bacterial cells during the PEC inactivation process. The decrease of protein concentration occurred very earlier in the PEC process, and the cytoplasmic protein leakage seems unlikely responsible, especially in the first 15 min considering a membrane did not permeabilize significantly until 15 min; so the loss of membrane associated proteins may occur at this stage.[43] Another reason may be that aggregation of proteins after PEC makes protein insoluble for extraction.[44] In contrast, the protein concentration reduction was not observed during the PC or EC processes, consistent with their poor bactericidal performance. To provide more details of the protein leakage, an SDS-PAGE experiment was conducted with extracted protein from treated cells (10^8 CFU mL^{-1}) (Figure 5). Proteins with molecular weights ranging from 14.4 to 97.4 kDa were clearly observed for the initial sample, and the dominant protein species were found to be between 42.7 and 31.0 kDa. However, during PEC treatment, the protein band intensities showed obvious time-dependent, gradual weakening. For example, all the bands exhibited lower intensity at 2 h compared with the untreated sample, and only the protein of ∼42.7 kDa could be observed after 3 h treatment, then fading at 5 h. Both intracellular and extracellular ROSs may oxidize the protein side chains, especially lysine, arginine, and threonine, to generate carbonyl groups.[45] Therefore, the protein carbonyl level was monitored in order to assess the oxidative damage to proteins in the PEC system, with a bacterial suspension of 10^8 CFU mL^{-1} (Figure 6). During the first hour, the protein concentration did not decrease, and the protein carbonyl level was still relatively low, which suggested that the bacteria maintained effective defending capacity against the oxidative stress. However, the protein oxidation was accelerated after 1 h, implying that the defending enzymes such as CAT and SOD were inactivated by ROSs and the proteins were oxidatively damaged.[14] Nevertheless, during PC and EC treatments, the proteins kept their bands, as well as intensities, with little changes within 8-h treatment intervals. It was reported that proteins tended to be oxidized and aggregate after solar irradiation, probably through ROSs generation.[44] Considering the ROSs mediated bacterial inactivation mechanism in PEC and the elevated protein oxidation level,

dx.doi.org/10.1021/es502471h | Environ. Sci. Technol. 2014, 48, 9412−9419

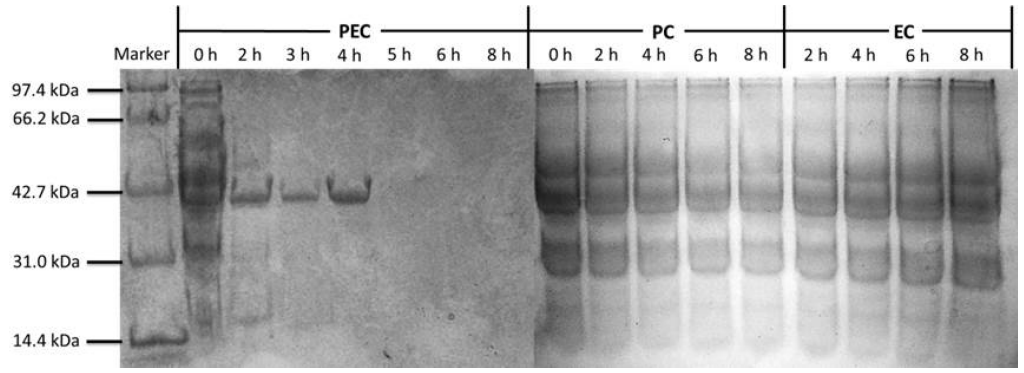

Figure 5. SDS-PAGE detection of protein content in cell lysate during PEC, PC, and EC inactivation of *E. coli* within 0, 2, 4, 6, and 8 h, respectively. The initial bacterial concentration was 10^8 CFU mL^{-1}.

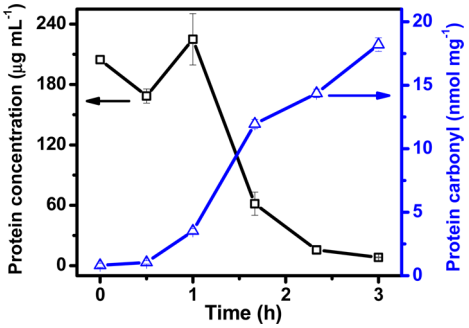

Figure 6. Determination of protein concentration (□) in 120 μL concentrated cell lysate from 5 mL bacterial suspension and the protein carbonyl level (Δ) during PEC inactivation. The initial bacterial concentration was 10^8 CFU mL^{-1}.

aggregation seems quite possible as a direct consequence of protein oxidation. Nevertheless, this inference needs further studies.

Leakage or oxidative damage of proteins may not be completely lethal to the bacteria, as self-repair and regrowth will take place under the right conditions.[46] Comparatively, the severe damage or loss of another bacterial building block, DNA, especially the chromosomal DNA, would cause definite bacterial death. Therefore, the influence of PEC treatment on bacterial DNA was studied in order to determine the cause of bacterial death from a genomic point of view such as DNA leakage or damage (Figure 7). Fluorescent intensity of the bands corresponding to genomic DNA extracted from the processed bacterial cells decreased within 2 h of PEC inactivation, implying the leakage of genomic DNA. The chromosomal DNA continued fading thereafter, and the DNA band completely disappeared after 5 h of treatment. Furthermore, the electrophoretic mobility of the observed genomic DNA bands increased slightly when PEC treatment was prolonged, which may indicate the decomposing of chromosomal DNA caused by PEC. In contrast, the leakage of genomic DNA from *E. coli* cells was not observed in either PC or EC systems.

TOC concentration changes in the bacterial suspension were further investigated to understand the decomposition and mineralization of bacteria cells during PEC treatment. As shown in Figure S12, the TOC content of 10^7 CFU mL^{-1} suspension was reduced by ~50% within 5 h of PEC treatment, indicating that the mineralization of the bacterial building blocks, such as leaked proteins and DNA, was realized during the PEC process.

Given the results of the above systematic investigation on the inactivation process, an in-depth understanding of the PEC inactivation mechanism of bacteria is proposed. First of all, the ROSs produced by UV illuminated nanotubular TiO_2 was responsible for the PEC bacteria inactivation, among which H_2O_2 was demonstrated to be the major disinfectant with the capacity to diffuse into bulk suspension and across bacterial membranes. At the beginning, ROSs was partly quenched by bacterial antioxidative enzymes, such as SOD and CAT. Nevertheless, ROSs could gradually inactivate CAT and SOD, which subsequently caused fast accumulation of ROSs. The ROSs then attacked bacterial membranes, which led to the loss of membrane integrity, followed by the leakage of cytoplasm. Longer PEC treatment would result in the decomposition of

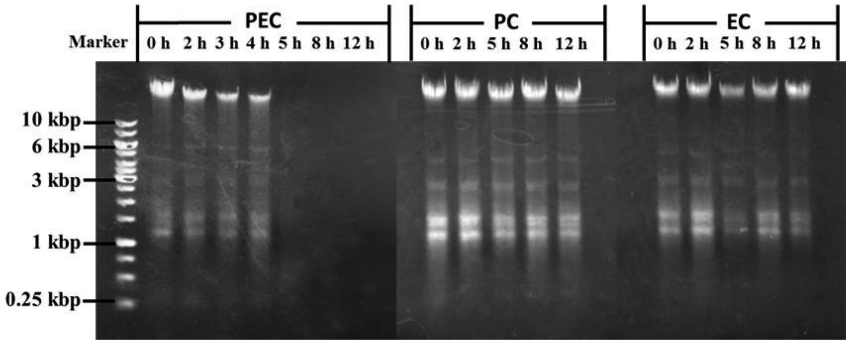

Figure 7. Investigation of leakage and damage of bacterial genomic DNA extracted from harvested cells during PEC, PC, and EC processes by means of agarose gel electrophoresis. The initial bacterial concentration was 10^8 CFU mL^{-1}.

dx.doi.org/10.1021/es502471h | *Environ. Sci. Technol.* 2014, 48, 9412–9419

the bacterial envelope and faster leakage of cytoplasmic content, especially biomolecules such as proteins and DNA. Finally, the leaked substances and cell debris are further degraded and mineralized during prolonged treatment.

■ ASSOCIATED CONTENT

Supporting Information

The diagram of the experimental apparatus, the protocols for anode preparation, DCFH-DA test, SEM sample preparation, and enzyme activity assay. This material is available free of charge via the Internet at http://pubs.acs.org.

■ AUTHOR INFORMATION

Corresponding Author

*Phone: +86-20-85291501. Fax: +86-20-85290706. E-mail: antc99@gig.ac.cn.

Notes

The authors declare no competing financial interest.

■ ACKNOWLEDGMENTS

This is contribution No. IS-1927 from GIGCAS. This work was supported by NSFC (41373103 and 21077104), Research Grant Council, Hong Kong SAR Government (476811), and Earmarked Fund of SKLOG (SKLOG2011A02).

■ REFERENCES

(1) Sketchell, J.; Peterson, H. G.; Christofi, N. Disinfection by-product formation after biologically assisted GAC treatment of water-supplies with different bromide and DOC content. *Water Res.* **1995**, *29* (12), 2635−2642, DOI: 10.1016/0043-1354(95)00130-D.

(2) Kulkarni, P.; Chellam, S. Disinfection by-product formation following chlorination of drinking water: Artificial neural network models and changes in speciation with treatment. *Sci. Total Environ.* **2010**, *408* (19), 4202−4210, DOI: 10.1016/j.scitotenv.2010.05.040.

(3) Matsunaga, T.; Tomoda, R.; Nakajima, T.; Wake, H. Photoelectrochemical sterilization of microbial cells by semiconductor powders. *FEMS Microbiol. Lett.* **1985**, *29* (1−2), 211−214.

(4) Xia, D. H.; Ng, T. W.; An, T. C.; Li, G. Y.; Li, Y.; Yip, H. Y.; Zhao, H. J.; Lu, A. H.; Wong, P. K. A recyclable mineral catalyst for visible-light-driven photocatalytic inactivation of bacteria: Natural magnetic sphalerite. *Environ. Sci. Technol.* **2013**, *47* (19), 11166−11173, DOI: 10.1021/es402170b.

(5) Wang, W. J.; Yu, Y.; An, T. C.; Li, G. Y.; Yip, H. Y.; Yu, J. C.; Wong, P. K. Visible-light-driven photocatalytic inactivation of *E. coli* K-12 by bismuth vanadate nanotubes: Bactericidal performance and mechanism. *Environ. Sci. Technol.* **2012**, *46* (8), 4599−4606, DOI: 10.1021/es2042977.

(6) Li, Q.; Xie, R. C.; Ll, Y. W.; Mintz, E. A.; Shang, J. K. Enhanced visible-light-induced photocatalytic disinfection of *E-coli* by carbon-sensitized nitrogen-doped titanium oxide. *Environ. Sci. Technol.* **2007**, *41* (14), 5050−5056, DOI: 10.1021/es062753c.

(7) Cheng, Y. W.; Chan, R. C.; Wong, P. K. Disinfection of *Legionella pneumophila* by photocatalytic oxidation. *Water Res.* **2007**, *41* (4), 842−852, DOI: 10.1016/j.watres.2006.11.033.

(8) Shi, H. X.; Chen, J. Y.; Li, G.. Y.; Nie, X.; Zhao, H. J.; Wong, P. K.; An, T. C. Synthesis and characterization of novel plasmonic Ag/AgX-CNTs (X = Cl, Br, I) nanocomposite photocatalysts and synergetic degradation of organic pollutant under visible light. *ACS Appl. Mater. Interfaces* **2013**, *5* (15), 6959−6967, DOI: 10.1021/am401459c.

(9) Kozlova, E. A.; Safatov, A. S.; Kiselev, S. A.; Marchenko, V. Y.; Sergeev, A. A.; Skarnovich, M. O.; Emelyanova, E. K.; Smetannikova, M. A.; Buryak, G. A.; Vorontsov, A. V. Inactivation and mineralization of aerosol deposited model pathogenic microorganisms over TiO_2 and Pt/TiO_2. *Environ. Sci. Technol.* **2010**, *44* (13), 5121−5126, DOI: 10.1021/es100156p.

(10) Cho, M.; Chung, H.; Choi, W.; Yoon, J. Linear correlation between inactivation of *E. coli* and OH radical concentration in TiO_2 photocatalytic disinfection. *Water Res.* **2004**, *38* (4), 1069−1077, DOI: 10.1016/j.watres.2003.10.029.

(11) Cho, M.; Chung, H. M.; Choi, W. Y.; Yoon, J. Y. Different inactivation behaviors of MS-2 phage and *Escherichia coli* in TiO_2 photocatalytic disinfection. *Appl. Environ. Microbiol.* **2005**, *71* (1), 270−275, DOI: 10.1128/AEM.71.1.270-275.2005.

(12) Kikuchi, Y.; Sunada, K.; Iyoda, T.; Hashimoto, K.; Fujishima, A. Photocatalytic bactericidal effect of TiO_2 thin films: Dynamic view of the active oxygen species responsible for the effect. *J. Photochem. Photobiol., A* **1997**, *106* (1−3), 51−56, DOI: 10.1016/S1010-6030(97)00038-5.

(13) Wang, W. J.; Zhang, L. Z.; An, T. C.; Li, G. Y.; Yip, H. Y.; Wong, P. K. Comparative study of visible-light-driven photocatalytic mechanisms of dye decolorization and bacterial disinfection by B−Ni-codoped TiO_2 microspheres: The role of different reactive species. *Appl. Catal., B* **2011**, *108−109* (0), 108−116, DOI: 10.1016/j.apcatb.2011.08.015.

(14) Suryo Rahmanto, A.; Pattison, D. I.; Davies, M. J. Photo-oxidation-induced inactivation of the selenium-containing protective enzymes thioredoxin reductase and glutathione peroxidase. *Free Radical Biol. Med.* **2012**, *53* (6), 1308−1316, DOI: 10.1016/j.freeradbiomed.2012.07.016.

(15) Hirakawa, K.; Mori, M.; Yoshida, M.; Oikawa, S.; Kawanishi, S. Photo-irradiated titanium dioxide catalyzes site specific DNA damage via generation of hydrogen peroxide. *Free Radical Res.* **2004**, *38* (5), 439−447, DOI: 10.1080/10715760420002064487.

(16) Pigeot-Rémy, S.; Simonet, F.; Atlan, D.; Lazzaroni, J. C.; Guillard, C. Bactericidal efficiency and mode of action: A comparative study of photochemistry and photocatalysis. *Water Res.* **2012**, *46* (10), 3208−3218, DOI: 10.1016/j.watres.2012.03.019.

(17) Hu, C.; Guo, J.; Qu, J.; Hu, X. Photocatalytic degradation of pathogenic bacteria with AgI/TiO_2 under visible light irradiation. *Langmuir* **2007**, *23* (9), 4982−4987, DOI: 10.1021/la063626x.

(18) Lu, Z. X.; Zhou, L.; Zhang, Z. L.; Shi, W. L.; Xie, Z. X.; Xie, H. Y.; Pang, D. W.; Shen, P. Cell damage induced by photocatalysis of TiO_2 thin films. *Langmuir* **2003**, *19* (21), 8765−8768, DOI: 10.1021/la034807r.

(19) Li, G. Y.; Liu, X. L.; Zhang, H. M.; An, T. C.; Zhang, S. Q.; Carroll, A. R.; Zhao, H. J. In situ photoelectrocatalytic generation of bactericide for instant inactivation and rapid decomposition of Gram-negative bacteria. *J. Catal.* **2011**, *277* (1), 88−94, DOI: 10.1016/j.jcat.2010.10.011.

(20) Nie, X.; Li, G. Y.; Gao, M. H.; Sun, H. W.; Liu, X. L.; Zhao, H. J.; Wong, P. K.; An, T. C. Comparative study on the photoelectrocatalytic inactivation of *Escherichia coli* K-12 and its mutant Escherichia coli BW25113 using TiO_2 nanotubes as a photoanode. *Appl. Catal., B* **2014**, *147*, 562−570, DOI: 10.1016/j.apcatb.2013.09.037.

(21) Baram, N.; Starosvetsky, D.; Starosvetsky, J.; Epshtein, M.; Armon, R.; Ein-Eli, Y. Enhanced photo-efficiency of immobilized TiO_2 catalyst via intense anodic bias. *Electrochem. Commun.* **2007**, *9* (7), 1684−1688, DOI: 10.1016/j.elecom.2007.03.017.

(22) Shankar, K.; Basham, J. I.; Allam, N. K.; Varghese, O. K.; Mor, G. K.; Feng, X. J.; Paulose, M.; Seabold, J. A.; Choi, K. S.; Grimes, C. A. Recent advances in the use of TiO_2 nanotube and nanowire arrays for oxidative photoelectrochemistry. *J. Phys. Chem. C* **2009**, *113* (16), 6327−6359, DOI: 10.1021/jp809385x.

(23) Nie, X.; Chen, J. Y.; Li, G. Y.; Shi, H. X.; Zhao, H. J.; Wong, P. K.; An, T. C. Synthesis and characterization of TiO_2 nanotube photoanode and its application in photoelectrocatalytic degradation of model environmental pharmaceuticals. *J. Chem. Technol. Biotechnol.* **2013**, *88* (8), 1488−1497, DOI: 10.1002/jctb.3992.

(24) Shi, H. X.; Li, G. Y.; Sun, H. W.; An, T. C.; Zhao, H. J.; Wong, P. K. Visible-light-driven photocatalytic inactivation of E. coli by Ag/AgX-CNTs (X=Cl, Br, I) plasmonic photocatalysts: Bacterial performance and deactivation mechanism. *Appl. Catal., B* **2014**, *158−159*, 301−307, http://dx.doi.org/10.1016/j.apcatb.2014.04.033.

(25) Nie, X.; Li, G. Y.; Wong, P. K.; Zhao, H. J.; An, T. C. Synthesis and characterization of N-doped carbonaceous/TiO_2 composite photoanodes for visible-light photoelectrocatalytic inactivation of *Escherichia coli* K-12. *Catal. Today* **2014**, *230*, 67−73, DOI: 10.1016/j.cattod.2013.09.046.
(26) Royall, J. A.; Ischiropoulos, H. Evaluation of 2′,7′-dichlorofluorescin and dihydrorhodamine 123 as fluorescent-probes for intracellular H_2O_2 in cultured endothelial-cells. *Arch. Biochem. Biophys.* **1993**, *302* (2), 348−355, DOI: 10.1006/abbi.1993.1222.
(27) Li, G. Y.; Liu, X. L.; Zhang, H. M.; Wong, P. K.; An, T. C.; Zhao, H. J. Comparative studies of photocatalytic and photoelectrocatalytic inactivation of *E. coli* in presence of halides. *Appl. Catal., B* **2013**, *140*−*141*, 225−232, DOI: 10.1016/j.apcatb.2013.04.004.
(28) Vatansever, F.; de Melo, W. C.; Avci, P.; Vecchio, D.; Sadasivam, M.; Gupta, A.; Chandran, R.; Karimi, M.; Parizotto, N. A.; Yin, R.; Tegos, G. P.; Hamblin, M. R. Antimicrobial strategies centered around reactive oxygen species–bactericidal antibiotics, photodynamic therapy, and beyond. *FEMS Microbiol. Rev.* **2013**, *37* (6), 955−989, DOI: 10.1111/1574-6976.12026.
(29) Luo, W.; Abbas, M. E.; Zhu, L. H.; Deng, K. J.; Tang, H. Q. Rapid quantitative determination of hydrogen peroxide by oxidation decolorization of methyl orange using a Fenton reaction system. *Anal. Chim. Acta* **2008**, *629* (1−2), 1−5, DOI: 10.1016/j.aca.2008.09.009.
(30) Gumy, D.; Morais, C.; Bowen, P.; Pulgarin, C.; Giraldo, S.; Hajdu, R.; Kiwi, J. Catalytic activity of commercial of TiO2 powders for the abatement of the bacteria (*E-coli*) under solar simulated light: Influence of the isoelectric point. *Appl. Catal., B* **2006**, *63* (1−2), 76−84, DOI: 10.1016/j.apcatb.2005.09.013.
(31) Baram, N.; Starosvetsky, D.; Starosvetsky, J.; Epshtein, M.; Armon, R.; Ein-Eli, Y. Photocatalytic inactivation of microorganisms using nanotubular TiO_2. *Appl. Catal., B* **2011**, *101* (3−4), 212−219, DOI: 10.1016/j.apcatb.2010.09.024.
(32) Rohnstock, A.; Lehmann, L. Evaluation of the probe dihydrocalcein acetoxymethylester as an indicator of reactive oxygen species formation and comparison with oxidative DNA base modification determined by modified alkaline elution technique. *Toxicol. in Vitro* **2007**, *21* (8), 1552−1562, DOI: 10.1016/j.tiv.2007.05.001.
(33) Gogniat, G.; Dukan, S. TiO_2 photocatalysis causes DNA damage via fenton reaction-generated hydroxyl radicals during the recovery period. *Appl. Environ. Microbiol.* **2007**, *73* (23), 7740−7743, DOI: 10.1128/AEM.01079-07.
(34) Park, S.; Imlay, J. A. High levels of intracellular cysteine promote oxidative DNA damage by driving the Fenton reaction. *J. Bacteriol.* **2003**, *185* (6), 1942−1950, DOI: 10.1128/JB.185.6.1942-1950.2003.
(35) Farr, S. B.; Kogoma, T. Oxidative stress responses in *Escherichia-coli* and *Salmonella-typhimurium*. *Microbiol. Rev.* **1991**, *55* (4), 561−585.
(36) Storz, G.; Tartaglia, L. A.; Farr, S. B.; Ames, B. N. Bacterial defenses against oxidative stress. *Trends Genet.* **1990**, *6* (11), 363−368, DOI: 10.1016/0168-9525(90)90278-E.
(37) Kwon, H. Y.; Choi, S. Y.; Won, M. H.; Kang, T. C.; Kang, J. H. Oxidative modification and inactivation of Cu,Zn-superoxide dismutase by 2,2′-azobis(2-amidinopropane) dihydrochloride. *Biochim. Biophys. Acta, Protein Struct. Mol. Enzymol.* **2000**, *1543* (1), 69−76, DOI: 10.1016/S0167-4838(00)00197-7.
(38) Singh, S.; Brocker, C.; Koppaka, V.; Chen, Y.; Jackson, B. C.; Matsumoto, A.; Thompson, D. C.; Vasiliou, V. Aldehyde dehydrogenases in cellular responses to oxidative/electrophilic stress. *Free Radical Biol. Med.* **2013**, *56*, 89−101, DOI: 10.1016/j.freeradbiomed.2012.11.010.
(39) Dalrymple, O. K.; Stefanakos, E.; Trotz, M. A.; Goswami, D. Y. A review of the mechanisms and modeling of photocatalytic disinfection. *Appl. Catal., B* **2010**, *98* (1−2), 27−38, DOI: 10.1016/j.apcatb.2010.05.001.
(40) Berney, M.; Weilenmann, H.-U.; Egli, T. Flow-cytometric study of vital cellular functions in *Escherichia coli* during solar disinfection (SODIS). *Microbiology* **2006**, *152* (6), 1719−1729, DOI: 10.1099/mic.0.28617-0.
(41) Bosshard, F.; Bucheli, M.; Meur, Y.; Egli, T. The respiratory chain is the cell's Achilles' heel during UVA inactivation in *Escherichia coli*. *Microbiology* **2010**, *156* (7), 2006−2015, DOI: 10.1099/mic.0.038471-0.
(42) Zheng, H.; Maness, P. C.; Blake, D. M.; Wolfrum, E. J.; Smolinski, S. L.; Jacoby, W. A. Bactericidal mode of titanium dioxide photocatalysis. *J. Photochem. Photobiol., A* **2000**, *130* (2−3), 163−170.
(43) Carre, G.; Hamon, E.; Ennahar, S.; Estner, M.; Lett, M. C.; Horvatovich, P.; Gies, J. P.; Keller, V.; Keller, N.; Andre, P. TiO_2 photocatalysis damages lipids and proteins in *Escherichia coli*. *Appl. Environ. Microbiol.* **2014**, *80* (8), 2573−2581, DOI: 10.1128/AEM.03995-13.
(44) Bosshard, F.; Riedel, K.; Schneider, T.; Geiser, C.; Bucheli, M.; Egli, T. Protein oxidation and aggregation in UVA-irradiated *Escherichia coli* cells as signs of accelerated cellular senescence. *Environ. Microbiol.* **2010**, *12* (11), 2931−2945, DOI: 10.1111/j.1462-2920.2010.02268.x.
(45) Dalle-Donne, I.; Rossi, R.; Giustarini, D.; Milzani, A.; Colombo, R. Protein carbonyl groups as biomarkers of oxidative stress. *Clin. Chim. Acta* **2003**, *329* (1−2), 23−38, DOI: 10.1016/S0009-8981(03)00003-2.
(46) Leung, T. Y.; Chan, C. Y.; Hu, C.; Yu, J. C.; Wong, P. K. Photocatalytic disinfection of marine bacteria using fluorescent light. *Water Res.* **2008**, *42* (19), 4827−4837, DOI: 10.1016/j.watres.2008.08.031.